

# Radar cross section generation of the possible non-cooperative targets

Rudolf Palme

Department of Aircraft and Ships  
Budapest University of Technology and Economics  
Budapest, Hungary  
palme@rht.bme.hu

**Abstract**—This paper defines non-cooperative targets and presents a calculation method of their radar cross section also in bistatic cases. First a three-dimensional model is given which is built-up by triangular facets. From the available flight path the azimuth and elevation angles are determined to position the target model. Then simple shadowing algorithm has been used in order to have short computational time and acceptable accurate. The calculation of radar cross section uses physical optics theory. The surface integral is numerically evaluated over the illuminated surface only. Radar cross section has been calculated by summarizing the results of each triangle. This work is part of the EU FP6 SINBAD (Safety and security Improved by New functionality for Better Awareness on airport approach and departure Domain) project leading by THALES.

**Keywords:** *Non-cooperative Target (NCT), TNB Frame, Triangular Facet, Shadowing, Physical Optics (PO), RCS, Radar Cross Section*

## I. INTRODUCTION

Number of Non-Cooperative Targets (NCT) is increasing with growth of aviation, widely use of Unmanned Aerial Vehicle (UAV), future operation of personal air vehicles and adaptation of birds to high density of air transport. It is clear the non-cooperative targets may cause hazards and series emergency situations in air especially in airport regions. The needs in system can detect the NCTs and can predict possible hazard situations initiating by such targets are considerable increased especially after 9.11. The rate of the caused hazard depends on the target's technical parameters such as size, speed and maneuverability. Therefore it is highly recommended to classify NCTs. That was the reason why the European Commission started the Safety and security Improved by New functionality for Better Awareness on airport approach and departure Domain (SINBAD) project on the 1st of July, 2007. The scope for the SINBAD system covers the support of ATC Controllers (ATCO) for the awareness of Non-Cooperative Targets within the Controlled Terminal Region (CTR) and for the maintenance of the safety of air traffic (radar separation).

One of the main modules of SINBAD system is the NCT classification which aims to characterize the detected NCTs against a set of aircraft classes. On the one hand, the

classification method can be based on Radar Cross Section (RCS). Therefore the goal of this paper is developing RCS estimative algorithm at least to classify such targets but in optimal case to identify them.

## II. NON-COOPERATIVE TARGETS

Those flying objects which do not communicate with the Air Traffic Control/Air Traffic Management (ATC/ATM) service are called as non-cooperative targets. This means that the aircraft is not responding to the interrogation signal transmitted by the Secondary Surveillance Radar (SSR), since it has no radar transponder, or if so it is switch off or having a system failure. So any flying object such as bird, UAV, hang glider, aircraft with failure in its communication system, small aircraft, terrorist's aircraft, etc. can be possible non-cooperative target.

In 2007, the number of the European non-cooperative targets is increasing [1]; the prediction to year 2020 is given in Fig. 1. The major reasons of this augmentation include the followings:

- the growth of the traditional air traffic that – having approximately equal system reliabilities – leads to a higher probability of an aircraft radio communication, or other fail that results in a non-cooperative flight,
- the enlargement of the unmanned aerial vehicles,
- the presents of the recreational flights (e.g. hang gliders, balloons),
- the appearance of the personal small aircraft (for a maximum of 6 passengers), which being designed to be accessible to common / ordinary people, might even be flown by pilots with limited experience,
- or the existence of birds at low altitudes.

The NCTs can cause hazards (decreasing in safety), conflicts and serious emergency situations (following with incidents or accidents). Therefore the new actual problem and task can be defined as the recognition, and identification of the non-cooperative targets and hazards in this way avoiding the emergency situations.

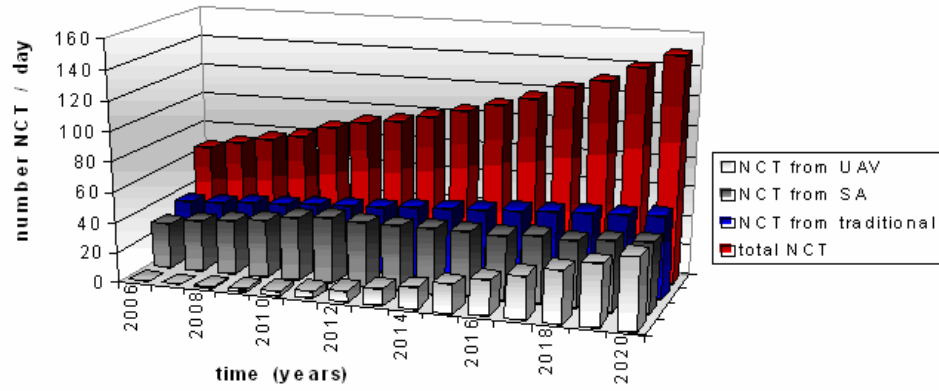


Figure 1. The evolution of the number of the European non-cooperative flights between 2006 and 2020 [1].

### III. MODEL POSITIONING WITH USE OF FLIGHT PATH DATA

First of all some assumptions have been made, these are follows:

- flight is coordinated flight all the way,
- there are not any bank angle over 90 degrees in absolute value,
- the target behaves as a fixed wing aircraft,
- and it flies with zero angle of attack.

The calculation based on the past of the flight which curve thus its derivative is given in Earth-axis system. Tangent, normal, and binormal unit vectors ( $\underline{T}$ ,  $\underline{N}$ ,  $\underline{B}$ ) have been calculated by using Frenet-Serret formulas. The vector  $\underline{tr}$  is pointing from the radar transmitter to the target. For model positioning it is necessary to determine the Euler angles of the target. In first step only the x-y coordinates have been considered so a modified tangent unit vector ( $\underline{T}_{xy}$ ) has also been calculated. The angle between this ( $\underline{T}_{xy}$ ) and the x direction vector is the yaw angle.

After that the TNB frame and  $\underline{tr}$  have been rotated with negative yaw angle so  $\underline{T1}$ ,  $\underline{N1}$ ,  $\underline{B1}$ , and  $\underline{tr1}$  are given. Fig. 2 shows these vectors on a helical flight path. In this situation the pitch angle is between  $\underline{T1}$  and the x direction vector.

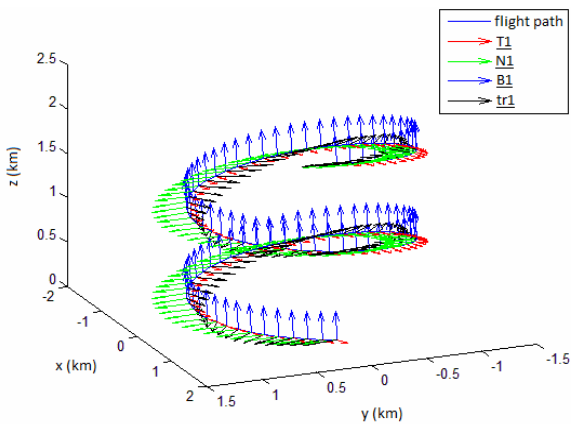


Figure 2. The flight path with rotated TNB frame.

Finally the bank angle has been determined if the radius of curvature ( $\underline{R}$ ) and the target's speed ( $\underline{v}$ ) are known as

$$bank = \arctan\left(\frac{v^2}{R}\right). \quad (1)$$

There are the azimuth and elevation angles of the target from the radar transmitter/receiver viewpoint between the inputs of the RCS calculation so it is also needed to calculate them. Now the  $\underline{T1}$ ,  $\underline{N1}$ ,  $\underline{B1}$ , and  $\underline{tr1}$  vectors have been rotated with negative pitch angle, the results are  $\underline{T2}$ ,  $\underline{N2}$ ,  $\underline{B2}$ , and  $\underline{tr2}$ . Because the original TNB frame was not considered the bank position, another rotation is necessary which rotate  $\underline{tr2}$  with (1) so  $\underline{tr3}$  is given. The projection of the radar beam in the x-y plane is

$$\underline{beamx} = \underline{tr3} - (\underline{tr3} * \underline{z}) * \underline{z} \quad (2)$$

where  $\underline{z}$  is the z direction vector. Afterwards the azimuth and elevation angles can be determined as

$$\phi = \pi - \arccos(\underline{T2} * \underline{beamx}) \quad (3)$$

if  $\underline{tr3}$  is directed along positive direction of y axis, otherwise

$$\phi = \pi + \arccos(\underline{T2} * \underline{beamx}), \quad (4)$$

$$\theta = \frac{\pi}{2} - \arccos(\underline{tr3} * \underline{beamx}) \quad (5)$$

if  $\underline{tr3}$  is directed along negative direction of z axis, otherwise

$$\theta = \frac{\pi}{2} + \arccos(\underline{tr3} * \underline{beamx}). \quad (6)$$

#### IV. MODEL PREPARATION, SHADOWING

##### A. Model preparation:

The models are given in Virtual Reality Modeling Language (VRML). VRML is a standard text file format for representing three-dimensional (3D) interactive vector graphics where, e.g., vertices and edges for a 3D polygon can be specified along with the surface color, UV mapped textures, shininess, transparency, and so on. Those models were considered which are built up by triangular facets only. The text file describes the 3D geometrical shape but no material properties because the RCS calculation contains implicit the perfect conducting material property valid for the whole model surface. Fig. 3 shows a generic airliner in accordance with the principles above.

The current excited on the surface of the scatterer is found by the tangential components of the incident fields on the surface. Since the fields exist only on the illuminated portions of the scattering body, the PO current for a conducting body is given by

$$\underline{J}^s = 2\underline{n}_f \times \underline{H}^i \quad (7)$$

in the illuminated region where  $\underline{n}_f$  is the unit normal vector of the surface positioned outward and  $\underline{H}^i$  is the magnetic field vector. In the shadow region the PO current is zero [2]. Thus it is an important step to determine which triangle in which region stands. In order that the shadowing calculation be simple and fast some assumption were considered that are follows:

- Only the midpoint of the triangles is analyzed instead of calculate overlap, because the surface of one triangle is negligible to the whole model.
- If there is a triangle between the analyzed midpoint and the radar transmitter, the triangle which owns the midpoint is located in the shadow region.

##### B. Shadowing:

The calculation has been made for every triangle. The first step is to define the triangle's geometric center as

$$\underline{midpoint1} = (\underline{P1} + \underline{P2} + \underline{P3}) / 3 \quad (8)$$

where  $\underline{P1}$ ,  $\underline{P2}$ ,  $\underline{P3}$  the position vectors of the triangle's vertices. The vector of the radar beam ( $\underline{r}$ ) has been defined as follows:

$$\underline{r} = \underline{midpoint1} - \underline{transm} \quad (9)$$

where  $\underline{transm}$  the position vector of the radar transmitter location. The nondirectional power density is – if the maximum of the transmitted power ( $peakpower$ ) is given – as in [3]:

$$power = \frac{peakpower}{4\pi * \underline{r}^2}. \quad (10)$$

Now every triangle has been considered in succession, until one has been found which is located between the radar transmitter ( $\underline{transm}$ ) and the center of the analyzed triangle (8). In case of exist a triangle of this kind it is shaded, otherwise it is illuminated. The analysis has been made for every triangle according to the next steps.

Label the vertices of the currently examined triangle to A, B and C. Constitute  $\underline{AB}$ ,  $\underline{BC}$  and  $\underline{CA}$  vectors. Calculate the normal vector of the surface of the triangle, and sign it with  $\underline{n}$ . Define the  $\underline{u}$  and  $\underline{w}$  vectors as follows:

$$\underline{u} = -\underline{r}, \quad (11)$$

$$\underline{w} = \underline{midpoint1} - \underline{A} \quad (12)$$

where  $\underline{A}$  is the position vector of vertex A. Create the next scalars:

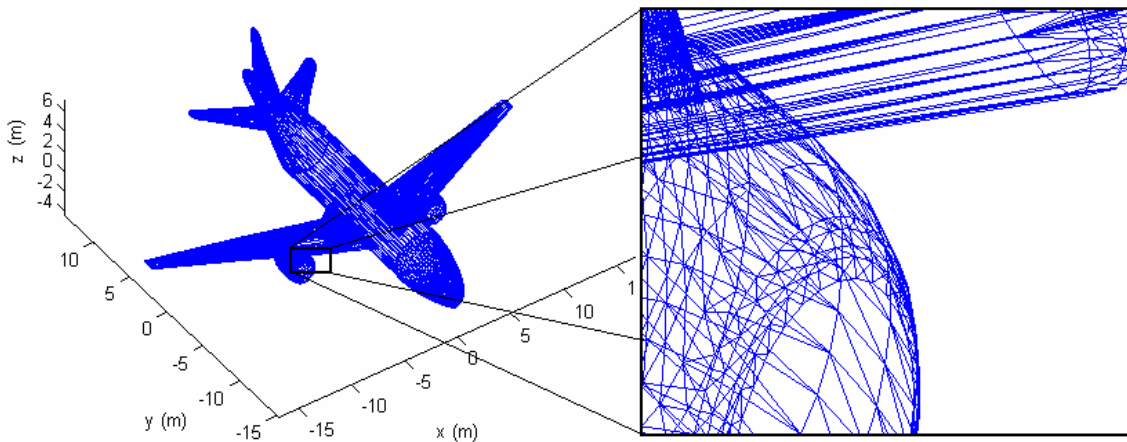


Figure 3. Generic airliner built-up by triangular facets.

$$D = \underline{n} * \underline{u}, \quad (13)$$

$$N = - \underline{n} * \underline{w}, \quad (14)$$

$$sI = \frac{N}{D}. \quad (15)$$

If the value (13) is close to zero (less than  $10^{-7}$ ), the surface of the analyzed triangle do not overlay the center of the other triangle. Otherwise the section of the analyzed dots intersects the surface if  $sI$  is between 0 and 1. In this case further analysis is needed to decide that the intersection is inside or outside the triangle because only inside case means shadowing. The position vector of intersection is

$$\underline{Intpoint} = \underline{midpoint1} + sI * \underline{u}. \quad (16)$$

Mark the sections between the A, B and C vertices and the dot of intersection with  $\underline{AP}$ ,  $\underline{BP}$  and  $\underline{CP}$ . So the intersection is inside the triangle if the next inequalities are true according to [4]:

$$0 < \underline{n} * (\underline{AB} \times \underline{AP}), \quad (17)$$

$$0 < \underline{n} * (\underline{BC} \times \underline{BP}), \quad (18)$$

$$0 < \underline{n} * (\underline{CA} \times \underline{CP}). \quad (19)$$

If overlaying has not been found, eventually it is necessary to analyze that the intersection is on the edge of the triangle (or have a maximum distance of  $10^{-4}$  m), and if it is there, it means shadowing also. First create the direction vector of the edge AB as

$$\underline{v1} = \frac{\underline{AB}}{|\underline{AB}|}. \quad (20)$$

The vector between the dot of intersection and the examined edge is

$$\underline{pr1} = \underline{Intpoint} - \underline{A}. \quad (21)$$

The distance of the edge's line and the dot of intersection is

$$\underline{tav1} = \left| (\underline{A} + (\underline{pr1} * \underline{v1}) * \underline{v1}) - \underline{Intpoint} \right|. \quad (22)$$

If (22) less than  $10^{-4}$  m it is necessary to examine that the section which contains the dot of intersection and which is perpendicular to the line of edge intersects it between the two vertices or not. Shadowing has been considered only the former case. The examination can be done as follows: In the equation of the edge's line the parameter of vertex A is known – it is zero – so only the parameter of vertex B has been calculated as

$$t1 = \frac{\underline{B} - \underline{A}}{\underline{v1}}. \quad (23)$$

It means shadowing if the next inequalities are true:

$$0 \leq \underline{pr1} * \underline{v1} \leq t1. \quad (24)$$

The analysis (20)-(24) has been done with the BC and CA edges also.

## V. COORDINATE TRANSFORMATIONS

Every triangle is located arbitrarily in a global coordinate system (x, y, z). In order to have the equations less complicated, a local coordinate system ( $x_l, y_l, z_l$ ) can be defined to each triangle with vertices A, B, C in order according to [5]. Let the triangle lie on the  $x_l - y_l$  plane in the newly defined local coordinate system. Put the origin of the local coordinate system at vertex A. Edge  $\underline{CA}$  has been taken along  $y_l$  axis. In this case the local coordinates are found using the following equations:

$$y_l = - \frac{\underline{CA}}{|\underline{CA}|}, \quad (25)$$

$$z_l = \frac{\underline{AB} \times (-\underline{CA})}{|\underline{AB} \times \underline{CA}|}, \quad (26)$$

$$x_l = y_l \times z_l. \quad (27)$$

The vector  $\underline{c_l}$  represents the distance between the global and local coordinate centers. Thus it is given as

$$\underline{c_l} = \underline{A} \quad (28)$$

where  $\underline{A}$  is the position vector of the vertex A. Now the transformation matrix can be defined for the global coordinate system to the local rectangular coordinate system as

$$\underline{\underline{m}}_1 = \begin{bmatrix} \underline{x}^* \underline{x}_l & \underline{x}^* \underline{y}_l & \underline{x}^* \underline{z}_l \\ \underline{y}^* \underline{x}_l & \underline{y}^* \underline{y}_l & \underline{y}^* \underline{z}_l \\ \underline{z}^* \underline{x}_l & \underline{z}^* \underline{y}_l & \underline{z}^* \underline{z}_l \end{bmatrix}. \quad (29)$$

The parametric expressions for edges AB and BC can be written in local coordinates as the following:

$$\alpha(x_l) = \alpha_0 + \alpha_1 x_l \quad (30)$$

$$\beta(x_l) = \beta_0 + \beta_1 x_l \quad (31)$$

Fig. 4 explains the labels in the equations above. Since vertex A is the origin of the local coordinate system, the parameters in (30) are given as

$$\alpha_0 = 0, \quad (32)$$

$$\alpha_1 = \frac{AB_{ly}}{AB_{lx}} \quad (33)$$

if  $AB_{lx} \neq 0$  otherwise

$$\alpha_1 = 0 \quad (34)$$

where  $\underline{AB}_l = \underline{AB}^* \underline{\underline{m}}_1$ , furthermore  $\underline{AB}_l$  indexing x and y refer to the first and second coordinate of the vector. Likewise the parameters in (31) are

$$\beta_0 = |\underline{CA}_l|, \quad (35)$$

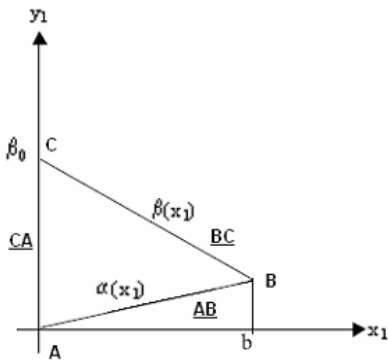


Figure 4. The triangle in local coordinates.

$$\beta_1 = -\frac{BC_{ly}}{|BC_{lx}|}. \quad (36)$$

The incident field given in the global rectangular coordinates should also be transformed into the local coordinate system with the transformation matrix  $\underline{\underline{m}}_1$ . It is necessary to transform the incident field from the rectangular local coordinate system to the spherical local coordinate system, in which calculations for the scattered field will be done. Fig. 5 shows the scattering configuration in global coordinate system.

Because the origins of the local rectangular and spherical coordinate systems are the same, the transformation matrix and its building-up vectors are found to be

$$\underline{\theta}_l^i = \begin{bmatrix} \cos \theta_l^i \cos \phi_l^i \\ \cos \theta_l^i \sin \phi_l^i \\ \sin \theta_l^i \end{bmatrix}, \quad (37)$$

$$\underline{\phi}_l^i = \begin{bmatrix} -\sin \phi_l^i \\ \cos \phi_l^i \\ 0 \end{bmatrix}, \quad (38)$$

$$\underline{\underline{m}}_2 = \begin{bmatrix} \underline{\theta}_l^i * \underline{x}_l & \underline{\phi}_l^i * \underline{x}_l \\ \underline{\theta}_l^i * \underline{y}_l & \underline{\phi}_l^i * \underline{y}_l \\ \underline{\theta}_l^i * \underline{z}_l & \underline{\phi}_l^i * \underline{z}_l \end{bmatrix}. \quad (39)$$

where  $\theta_l^i$  and  $\phi_l^i$  are the incident azimuth and elevation angles in local coordinates. In case of the backscattered beam the calculation is the same as above except for the angles of incidence are replaced by the angles of scattering:

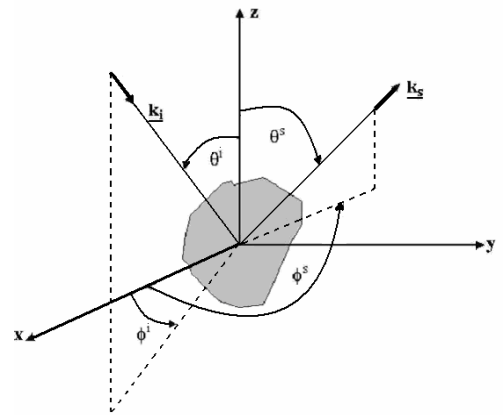


Figure 5. The scattering configuration.

$$\underline{\underline{m}}_3 = \begin{bmatrix} \underline{\theta}_l^s * \underline{x}_l & \underline{\phi}_l^s * \underline{x}_l \\ \underline{\theta}_l^s * \underline{y}_l & \underline{\phi}_l^s * \underline{y}_l \\ \underline{\theta}_l^s * \underline{z}_l & \underline{\phi}_l^s * \underline{z}_l \end{bmatrix} \quad (40)$$

## VI. PHYSICAL OPTICS (PO) FORMULATION

First the incident electric field has been calculated over the illuminated triangles one after the other. The electric field density is given after [6] by

$$einc = \sqrt{\eta * power} \quad (41)$$

where power comes from (10) and  $\eta$  is the intrinsic impedance of free space.

$$\eta = 120\pi \Omega \quad (42)$$

The propagation vector is given in spherical coordinates by (see Fig. 5)

$$\underline{k}_i = -(\underline{x} \sin \theta^i \cos \phi^i + \underline{y} \sin \theta^i \sin \phi^i + \underline{z} \cos \theta^i). \quad (43)$$

If the source illuminating the target is at a far enough distance, then the incident field can be taken as a plane wave. The incident electric and magnetic fields are given by the following expressions by [5]:

$$\underline{E}^i = \underline{E}_0^i e^{-j * k * \underline{k}_i * \underline{r}} \quad (44)$$

where  $\underline{k}_i$  and  $\underline{r}$  comes from (43) and (9),  $\underline{E}_0^i$  is the value of (41) with the direction  $\underline{k}_i$  and  $k$  is the wave number:

$$k = \frac{2\pi f}{c} \quad (45)$$

where  $c$  is the speed of light in vacuum and  $f$  is the frequency of the wave.

$$\underline{H}^i = \underline{H}_0^i e^{-j * k * \underline{k}_i * \underline{r}} \quad (46)$$

where

$$\underline{H}_0^i = \frac{1}{\eta} \underline{k}_i \times \underline{E}_0^i \quad (47)$$

To the RCS calculation some assumptions have been made these are summarized as follows:

- the solid models are built up from finite triangles,
- the whole model is created from the same conducting material,
- the models have rigid body,
- the distance between the radar and the target is large so the radar signals are perpendicular to each other and
- the analysis is static.

Thus the PO current for the models surface is given by (7). A plane wave of arbitrary polarization is incident from an angle  $(\theta_l^i, \phi_l^i)$ . The wave polarization is determined by the constants  $E_{\theta l}^i$  and  $E_{\phi l}^i$  in the expression

$$\underline{E}_l^i = (E_{\theta l}^i \underline{\theta}_l^i + E_{\phi l}^i \underline{\phi}_l^i) e^{-j * k * \underline{k}_i * \underline{r}_l} \quad (48)$$

where  $\underline{r}_l$  is the position vector of the even examined facet in spherical coordinates. The surface current induced on the +z side of the facet is given as

$$\underline{J}_l^s = \frac{2e^{-jk_l r_l}}{\eta} (\underline{x}_l (\cos \phi_l^i E_{\theta l}^i - \cos \theta_l^i \sin \phi_l^i E_{\phi l}^i) + \underline{y}_l (\sin \phi_l^i E_{\theta l}^i + \cos \theta_l^i \cos \phi_l^i E_{\phi l}^i)) \quad (49)$$

According to [7] if the position vector to a source point is  $\underline{p}'$  and the unit vector in the direction of the observation point is

$$\underline{p} = u \underline{x} + v \underline{y} + w \underline{z} \quad (50)$$

where  $u, v, w$  are the direction cosines of the observation point:

$$u = \sin \theta \cos \phi, \quad (51)$$

$$v = \sin \theta \sin \phi, \quad (52)$$

$$w = \cos \theta. \quad (53)$$

The components of the electric field tangential to a sphere at radius  $r$ , i.e. the radiation integrals are

$$E_{\theta}^s(x, y, z) = \frac{-jk\eta}{4r\pi} e^{-jkr} * \int \int \int_V (J_{\theta} * \underline{\theta} + \frac{1}{\eta} * J_m * \underline{\phi}) e^{jk \underline{p}' \cdot \underline{p}} dv' , \quad (54)$$

$$E_{\phi}^s(x, y, z) = \frac{-jk\eta}{4r\pi} e^{-jkr} * \int \int \int_V (J_{\phi} * \underline{\phi} - \frac{1}{\eta} * J_m * \underline{\theta}) e^{jk \underline{p}' \cdot \underline{p}} dv' \quad (55)$$

where  $J_m$  is the magnetic current and it is zero considered the assumptions. Using (49) in the (54) radiation integral gives with  $J_m = 0$  in the source point  $(x'_l, y'_l)$

$$E_{\theta}^s(x'_l, y'_l) = \frac{-jk\eta}{4\pi|r|} e^{-jk|r|} \int \int_s \frac{2e^{jkh}}{\eta} * \left[ (E_{0\theta} \cos \phi_l^i - E_{0\theta} \cos \theta_l^i \sin \phi_l^i) \cos \theta_l^s \cos \phi_l^s + (E_{0\theta} \sin \phi_l^i + E_{0\theta} \cos \theta_l^i \cos \phi_l^i) \cos \theta_l^s \sin \phi_l^s \right] e^{jkg} dx_l dy_l \quad (56)$$

where

$$h = x'_l \sin \theta_l^i \cos \phi_l^i + y'_l \sin \theta_l^i \sin \phi_l^i , \quad (57)$$

$$g = x'_l \sin \theta_l^s \cos \phi_l^s + y'_l \sin \theta_l^s \sin \phi_l^s . \quad (58)$$

With the assumptions (56) is

$$E_{\theta}^s(x'_l, y'_l) = \frac{-jk\eta}{4\pi|r|} e^{-jk|r|} \frac{2}{\eta} \int \int_s e^{jkh} * e^{jkg} dx_l dy_l * \left[ (E_{0\theta} \cos \phi_l^i - E_{0\theta} \cos \theta_l^i \sin \phi_l^i) \cos \theta_l^s \cos \phi_l^s + (E_{0\theta} \sin \phi_l^i + E_{0\theta} \cos \theta_l^i \cos \phi_l^i) \cos \theta_l^s \sin \phi_l^s \right] . \quad (59)$$

Similarly

$$E_{\phi}^s(x'_l, y'_l) = \frac{-jk\eta}{4\pi|r|} e^{-jk|r|} \frac{2}{\eta} \int \int_s e^{jkh} * e^{jkg} dx_l dy_l * \left[ (-E_{0\theta} \cos \phi_l^i + E_{0\theta} \cos \theta_l^i \sin \phi_l^i) \sin \phi_l^s + (E_{0\theta} \sin \phi_l^i + E_{0\theta} \cos \theta_l^i \cos \phi_l^i) \cos \phi_l^s \right] . \quad (60)$$

These surface integrals can be analytically calculated over the triangular facets. The integral in itself is given as

$$I_0 = \int_{x_l=0}^b \int_{y_l=\alpha(x_l)}^{\beta(x_l)} e^{jk((\sin \theta_l^i \cos \phi_l^i + \sin \theta_l^s \cos \phi_l^s) x_l + (\sin \theta_l^i \sin \phi_l^i + \sin \theta_l^s \sin \phi_l^s) y_l)} dx_l dy_l . \quad (61)$$

The limits of the integration are the edges of the particular triangle. The expressions for the integral limits are (30)-(31) with constants (32) – (36) and

$$b = AB_{lx} . \quad (62)$$

The scattered field from a single triangle is given as

$$\underline{E}_l^s = E_{\theta}^s \underline{\theta}_l + E_{\phi}^s \underline{\phi}_l . \quad (63)$$

The well-known RCS formula is used to compute the RCS of the target

$$\sigma = \lim_{r \rightarrow \infty} 4\pi r^2 * \frac{|E_l^s|^2}{|E_l^i|^2} \quad (64)$$

The RCS results from each illuminated triangle are summed up, in order to find the total radar cross section. Fig. 6 shows the ideal and calculated monostatic scattering pattern for square with vertical polarization and with edge lengths of  $5\lambda$  where  $\lambda$  is the wavelength. Usually the frequency-independent quantity  $\frac{\sigma}{\lambda^2}$  is plotted rather than  $\sigma$ .

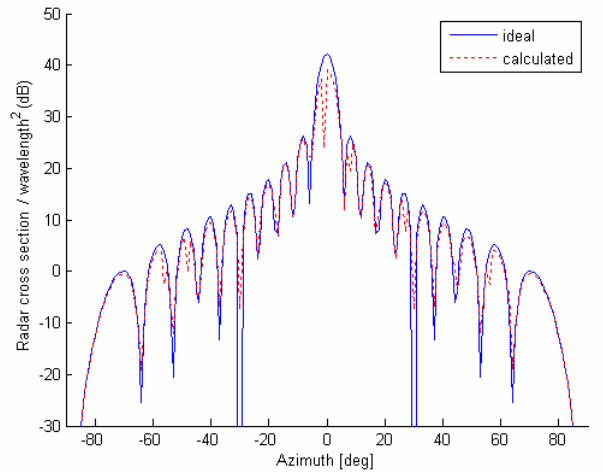


Figure 6. Ideal [7] and calculated radar cross section of square plate ( $\phi = 0$  deg).

Because the computational method is under development, it produces analytical errors in case of some special configuration (see on Fig. 6 the calculated graph) which are

- $\sin \theta_i^i \sin \phi_i^i + \sin \theta_i^s \sin \phi_i^s =$   
 $= \sin \theta_i^i \cos \phi_i^i + \sin \theta_i^s \cos \phi_i^s$  and  $\beta_1 = -1$
- or  $\beta_1 = \alpha_1$ .

It is possible to avoid these errors with another better coordinate transformation but the further examination is not scope of this paper. Besides the calculation method needs to accelerate, there is not any calculation with complex models which takes up a lot of time, only results from a hypothetical aircraft are given in Fig. 7.

## VII. CONCLUSION

The objective of this paper was to provide radar cross section calculation software to support the investigations of the EU sponsored SINBAD project, and to establish the background for further relevant research. Three dimensional VRML models were created built-up by triangular facets.

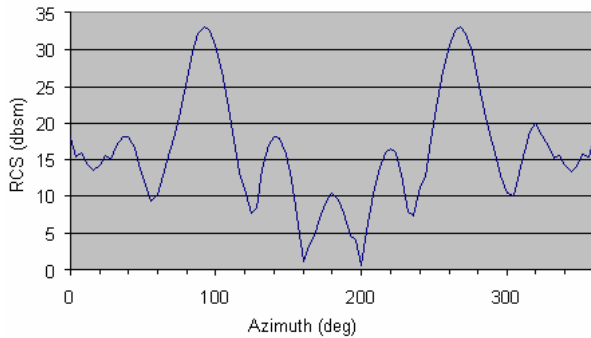


Figure 7. RCS diagram of a hypothetical aircraft at 10 GHz ( $\phi = 0$  deg).

The calculation based on these models as perfectly conducting solid models. Then the flight path was analyzed the Euler, azimuth and elevation angles were determined. To each triangle a ray tracing algorithm were applied that was developed to reach simple and fast computation time with acceptable accurate. PO integrals were formulated for each illuminated triangle which were calculated analytically. The radar cross section was summed up to get bistatic RCS from all possible viewpoint. The method presented in this paper is used by SINBAD Active Hazard Assessment (AHA) System to classify NCTs. The accurate of the results will be tested in Brno TMA (Terminal Control Area) with radar measurements in March of 2010 as scheduled.

The calculated data were reliable; the applied assumptions have imperceptible influence to the results. Note that the method needs further relevant development but the NCT classification is achievable with suitable 3D models and with calculation several different bistatic RCS pairs.

## REFERENCES

- [1] Dániel Rohács, "Prediction of the non-cooperative air targets at the European airport vicinities," Internal SINBAD Project Progress Report, unpublished.
- [2] Eugene F. Knott, John F. Shaeffer, Michael T. Tuley, "Radar cross section," Chapter 3, Artech House, 1985.
- [3] Merv C Budge, "Intro to radar systems," Chapter: Radar Range Equations, The University of Alabama in Huntsville, <http://www.ece.uah.edu/courses/material/EE619/index.htm>, 2005.
- [4] Iványi Antal (editor), "Algorithms of informatics," Chapter: Computer Graphics, Eötvös Kiadó, 2004.
- [5] N. A. Albayrak, "RCS computations with PO/PTD for conducting and impedance objects modelled as large flat plates," Bilkent University, unpublished.
- [6] John D. Jackson, "Classical electrodynamics third edition," John Wiley & Sons Inc., New York, 1998.
- [7] David C. Jenn, "Radar and laser cross section engineering second edition," Chapter 2, American Institute of Aeronautics and Astronautics Inc., Reston, 2005.